DOI: 10.1002/ejic.201100497

# Synthesis of Optically Active Ferrocene-Containing Platensimycin Derivatives with a C6–C7 Substitution Pattern

Malay Patra,[a] Gilles Gasser,[b] Michaela Wenzel,[c] Klaus Merz,[a] Julia E. Bandow,[c] and Nils Metzler-Nolte*[a]

**Keywords:** Bioinorganic chemistry / Sandwich complexes / Michael addition / Antibacterial agents / Planar chiral ferrocene / Platensimycin

Concurrently with the emergence of purely organic derivatives of the naturally occurring antibiotic platensimycin (**1a**), herein, we describe the design, synthesis and biological evaluation of both the enantiomers of a C6–C7 ferrocene-fused platensimycin derivative **2b**. ($S,S_P$)- and ($R,R_P$)-**2b** were prepared in nine steps starting from commercially available 4-ferrocenyl-4-oxobutyric acid via highly diastereoselective Michael additions of optically active planar-chiral ferrocene-fused cyclohexanone derivatives (**5**) with acrylate ester as the key step. Manual superimposition of ($S,S_P$)-**2b** on platensimycin bound to the active site of its target enzyme FabF suggests that the former fits nicely in the active site and the C6–C7-fused ferrocene occupies a pocket similarly to the C8–C9-fused tetracyclic cage of **1a**. Antimicrobial activities of ($S,S_P$)- and ($R,R_P$)-**2b** were tested against various Gram-positive and Gram-negative bacterial strains.

## Introduction

The recent discovery of the natural products platensimycin (**1a**, Figure 1)[1] and platencin (**1b**, Figure 1)[2] are important contributions to antibiotic research as both compounds display potent activity against Gram-positive pathogenic bacterial strains such as methicillin-resistant *Staphylococcus aureus* (MRSA) or vancomycin-resistant *Enterococcus faecalis*. While platensimycin only inhibits the FabF enzyme, platencin inhibits selectively both the FabH and FabF enzymes in the bacterial fatty acid biosynthesis. Although these two compounds are not suited to become drugs due to their poor pharmacokinetics, their unique mode of action, absence of cross-resistance to the existing antibiotics and inherent low toxicity profiles make them ideal lead structures for the development of novel synthetic derivatives with improved pharmacokinetics.[3]

Since their discoveries, numerous synthetic routes to **1a**, **1b** and related derivatives were reported and their antibacterial activities evaluated.[4] Nicolaou et al. reported two potent analogues, namely carba-platensimycin (**1e**, Figure 1) [4e] and adamanta-platensimycin (**1d**, Figure 1),[4c] which showed nearly similar antibacterial activity to **1a**/**1b**. Of note, some less or even inactive natural analogues such as platensimycin A1,[5] platensimycin B1–B4,[6] platensimide A, and platenin A1 were also recently identified, demonstrating that subtle changes can strongly influence the activity of the molecules. The recent structure-activity relationship (SAR) studies showed that any modification in the aromatic part leads to complete loss of the antibacterial activity. On the contrary, the tetracyclic cage is somewhat more tolerant to modifications.[7] A detailed structural comparison between different synthetic and natural analogues of **1a**/**1b** revealed that very small changes in the tetracyclic cage structures may

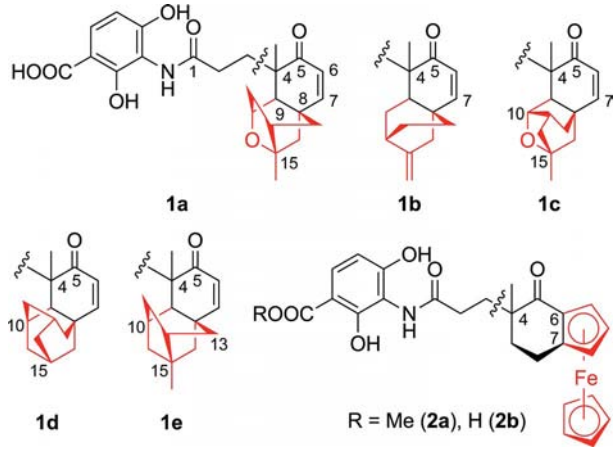


Figure 1. Structures of platensimycin (**1a**), lipophilic cage of platencin (**1b**), iso-platensimycin (**1c**), adamanta-platensimycin (**1d**), carba-platensimycin (**1e**) and of the chiral ferrocene-containing bioorganometallics (**2a** and **2b**) studied in this report.

[a] Lehrstuhl für Anorganische Chemie I, Bioanorganische Chemie, Fakultät für Chemie und Biochemie, Ruhr-Universität Bochum,
Universitätsstr. 150, 44801 Bochum, Germany
Fax: +49-234-3214378
E-mail: Nils.Metzler-Nolte@rub.de
[b] Institute of Inorganic Chemistry, University of Zürich, Winterthurerstrasse 190, 8057 Zürich, Switzerland
[c] Lehrstuhl für Biologie der Mikroorganismen, Fakultät für Biologie und Biotechnologie, Ruhr-Universität Bochum, Universitätsstr. 150, 44801 Bochum, Germany
Supporting information for this article is available on the WWW under http://dx.doi.org/10.1002/ejic.201100497.

  

also induce a dramatic change in the antibacterial activity. For example, in spite of very similar tetracyclic cage structure, iso-platensimycin (**1c**, Figure 1)[8] exhibits poor antibacterial activity against *S. aureus* compared to that of **1a**, whereas the two synthetic analogues, carba- and adamanta-platensimycin (**1e** and **1d**, Figure 1), lacking the ethereal oxygen were found to retain the antibacterial activity. These findings demonstrate that an isosteric substitution for the tetracyclic cage is potentially possible to achieve derivatives of **1a** with improved pharmacokinetics.

With this in mind, we have recently embarked on a project to investigate the possibility of replacing the complicated tetracyclic cage of **1a** by *organometallic* cores. The synthesis and biological evaluation of Cr-bioorganometallics based on the platensimycin lead structure was reported.[9] Our most active compound had a minimum inhibitory concentration (MIC) against *B. subtilis* of 80 μg/mL and was less potent than platensimycin, which has a MIC value of 0.2 μg/mL. Interestingly, however, its mode of action was found to be completely different from that of the parent compound.[10] This unexpected new mode of action might be interesting since the biomedical usefulness of **1a** and **1b** as a FabF enzyme inhibitor has been questioned. Recently, Brinster et al. reported that some Gram-positive pathogens might overcome the drug-induced inhibition of fatty acid biosynthesis in the presence of an external fatty acid source such as human serum,[11] although this does not seem to be true for *S. aureus*.[12]

We hence decided to further probe the opportunities inherent in metal derivatives of platensimycin. Ferrocene derivatives in particular have shown great promise in medicinal organometallic chemistry,[13] mainly due to their chemical stability, amenability to derivatization, and well-established redox chemistry. Prominent examples are found in the derivatization of existing drugs with ferrocene, mainly in anticancer and antimalarial research.[14] Probably the most successful example to date is ferroquine, a ferrocene derivative of the known antimalarial drug chloroquine, which was found to have improved activity against chloroquine-resistant *P. falciparum* strains.[15] Ferroquine has recently successfully passed clinical trial phase II and is now undergoing field testing. Our group recently reported the synthesis and biological evaluation of four ferrocene-containing bioorganometallics inspired by the antibiotic platensimycin lead structure. One of them having a 1,3-diferrocenoyl functionality was found to inhibit *S. aureus* growth at a MIC of 128 μg/mL.[16]

Taking this concept one step further, we have employed, in this study, a lipophilic and nearly isosteric chiral ferrocene-fused cyclohexenone derivative **4** (see Scheme 1) to design the platensimycin (**1a**) derivative **2b** (see Figure 1).[17] Compound **2b** is important no only because it allowed introducing chirality into our bioorganometallic design, but also because, unlike most previous derivatives of **1a** which focused on C8–C9 substitution, the proposed compounds will enhance the chemical space by probing the influence of C6–C7 substitution. Indeed, very recently, it has been shown that lipophilic substitution in the tetracyclic enone unit of **1a** led to compounds (7-phenyl- and 11-methyl-7-phenyl-platencimycin) with one fold improved antibacterial activity.[18] We chose C6–C7-fused ferrocene cyclohexenone **4** due to its facile accessibility, ease of further derivatizations and well-developed stereoselective transformations.[19] Additionally, as shown in Figure 2, manual superimposition of ($S$,$S_P$)-**2b** on platensimycin bound to the active site of its target enzyme FabF suggests that the former fits nicely in the active site and the C6–C7-fused ferrocene occupies a pocket similarly to the C8–C9-fused tetracyclic cage of **1a** (see Figure 2, b). We therefore expected that **2b** will provide crucial information on the effect of steric bulk at the C6–C7 position instead of the C8–C9 position on the biological activity of **1a/1b**. This has, to the best of our knowledge, not yet been examined. To this end, we report herein the synthesis and biological evaluations of racemic and optically pure chiral ferrocene-containing bioorganometallics (**2a** and **2b**, Figure 1) based on the lead structures of **1a/1b**. The compounds described herein enhance the chemical space for SAR studies on platensimycin derivatives.

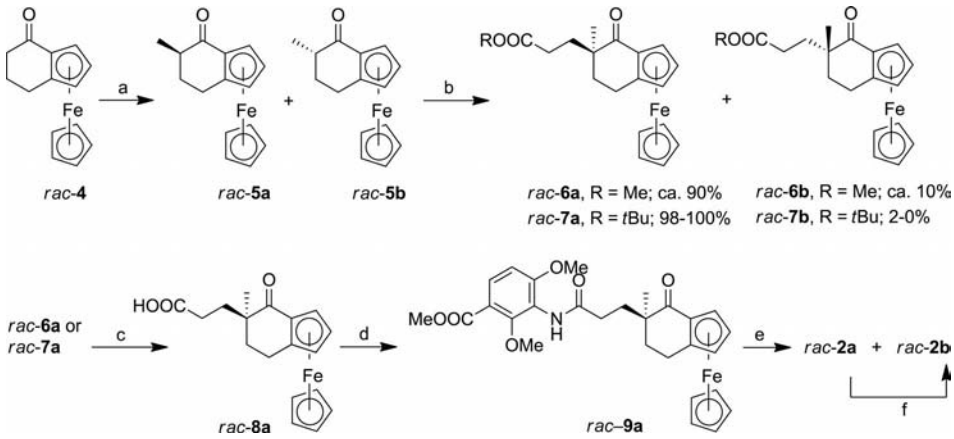


Scheme 1. Synthesis of *rac*-**2b**. Reagents and conditions: a) KHMDS, HMPA, MeI, THF, 76%; b) KO*t*Bu, methyl/*tert*-butyl acrylate, *t*BuOH, $Et_2O$, 61% for **6a** and **6b**, 81% for **7a**; c) 1 M aq. NaOH, MeOH/THF, 93%; d) methyl 3-amino-2,4-dimethoxybenzoate, HATU, DIPEA, DMF, 89%; e) $BBr_3$, $CHCl_3$; f) 1 M NaOH, MeOH/THF, $N_2$ atmosphere, 79% after two steps.

  

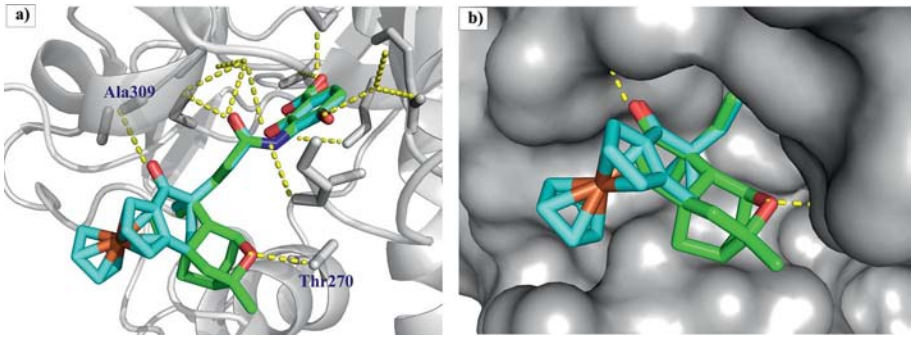


Figure 2. a) Superimposition of compound ($S,S_P$)-**2b** (cyan) on platensimycin (green) in the binding site of FabF; b) surface model showing the pocket for C6–C7-fused ferrocene in ($S,S_P$)-**2b**. Atomic coordinates for ($S,S_P$)-**2b** were obtained from the X-ray single crystal structure of *rac*-**2b**. The model obtained was manually fitted into the reported X-ray crystal structure of FabF (PDB code 2gfx).[1]

## Results and Discussion

### Synthesis and Characterization

The synthetic strategy to obtain *rac*-**2b** is outlined in Scheme 1. Treatment of *rac*-**4**[20] with KHMDS and MeI gave exclusively the *exo*-methylated ketone *rac*-**5a** together with the chromatographically inseparable *endo*-epimer *rac*-**5b** (≤ 10%). *rac*-**5a** can easily be purified by recrystalization from pentane (see Figure S7 in the Supporting Information for the single crystal structure of *rac*-**5a**).

Nonetheless, a pure product is not necessary to undergo the next synthetic step since epimerization occurs anyway. Thus, the diastereomeric mixture was subjected to base-catalyzed Michael addition to alkyl (Me and *t*Bu) acrylates. In our first attempt, the Michael addition of the mixture of *rac*-**5a** and *rac*-**5b** to methyl acrylate in presence of potassium *tert*-butoxide (KO*t*Bu) led to the formation of the epimeric mixture of *rac*-**6a** and *rac*-**6b** in 61% combined yield (Scheme 1). Trace amounts of *rac*-**7a** or **7b** together with two unknown impurities were also formed as side products. After purification by flash column chromatography, $^1$H NMR spectroscopy of the chromatographically inseparable mixture of *rac*-**6a** and *rac*-**6b** showed two singlets at $\delta$ = 1.23 ppm and 1.11 ppm. By analogy to previously reported chemical shifts of the *exo* and *endo* methyl group in 1,2-(α-keto-β-methyl-β-phenyltetramethylene)ferrocene[21] and 1,2-(α-keto-β-dimethyltetramethylene)ferrocene[22] as well as the $^1$H NMR spectrum obtained from the pure *rac*-**6a** after crystallization (see Figure S8 in the Supporting Information for the single crystal structure of *rac*-**6a**) from diethyl ether and pentane mixture, the singlets at $\delta$ = 1.23 and 1.11 ppm were assigned to the β-Me group signal from *rac*-**6a** and *rac*-**6b**, respectively (see Figure S10). The ratio of *rac*-**6a** and *rac*-**6b** in the mixture was calculated to be nearly 9:1 (ratio may slightly vary with the scale of the reaction). The high degree of diastereoselectivity during the Michael addition originates from the less hindered *exo*-face approach of the electrophile. However, when using *t*Bu acrylate, the Michael addition proceeded even more cleanly (only one spot in its TLC) with enhanced diastereoselectivity. After purification by column chromatography, *rac*-**7a** was obtained in 81% yield and the $^1$H NMR spectrum showed two singlets at $\delta$ = 1.39 and 1.23 ppm corresponding to the *t*Bu and β-Me groups of *rac*-**7a**, respectively. The absence of the singlet at $\delta$ = 1.11 ppm unambiguously proved the absence of minor diastereomer *rac*-**7b** within the $^1$H NMR detection limit (1-3%) (see Figure S10). Treatment of *rac*-**6a** or *rac*-**7a** with aqueous NaOH yielded the desired carboxylic acid *rac*-**8a** in quantitative yield. Alternatively, pure *rac*-**8a** can also be obtained by treatment of the mixture of *rac*-**6a** and *rac*-**6b**, with aqueous NaOH followed by only one recrystalization from a chloroform/ethyl acetate mixture. The single X-ray crystal structure of the *rac*-**8a** was also determined (see Figure S9). The carboxylic acid *rac*-**8a** was coupled with methyl 3-amino-2,4-dimethoxybenzoate using standard HATU mediated amide coupling and *rac*-**9a** was isolated in 89% yield (Scheme 1).[23] Finally, treatment of *rac*-**9a** with $BBr_3$ afforded completely deprotected *rac*-**2b**, together with partially deprotected *rac*-**2a** which can be easily converted into *rac*-**2b** by treatment with aqueous NaOH. The $^1$H NMR spectrum of *rac*-**2b** showed a singlet at $\delta$ = 1.32 ppm corresponding to the β-Me group together with all the other signals as expected. A clean peak at *m*/*z* 489.96 assigned to [**2b**–H]$^-$ was observed in the ESI-MS (neg. detection mode) spectrum. Furthermore, the single X-ray crystal structure of *rac*-**2b** was determined (Figure 3). Both the phenolic OH were found to be hydrogen bonded intramolecularly to the CO of the carboxylic acid and the amide group, respec-

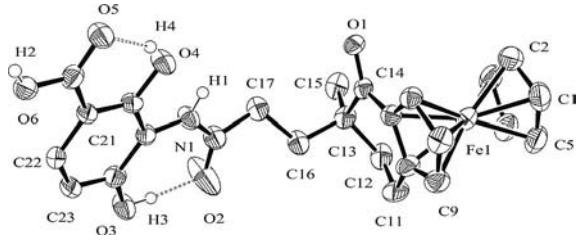


Figure 3. ORTEP plot of *rac*-**2b** [only the ($R,R_P$) isomer is shown and ellipsoids drawn at 50% probability level]. Hydrogen atoms are omitted for clarity. Selected bond lengths [Å] and angles [°]: Fe(1)–centroid Cp(C1–5) 1.653, Fe(1)–centroid Cp(C6–10) 1.632, average Fe–C Cp's 2.041(5), C(6)–C(14) 1.451(6), C(10)–C(11) 1.484(6), C(14)–C(13)–C(16) 105.5(3), C(12)–C(13)–C(16) 108.6(4), C(15)–C(13)–C(16) 112.3(4), C(14)–C(6)–Fe(1) 123.6(3), C(11)–C(10)–Fe(1) 125.3(3).

  

tively. The asymmetric unit contains two molecules, ($S$,$S_P$)-**2b** and ($R$,$R_P$)-**2b**, which are strongly hydrogen bonded with each other by three intermolecular hydrogen bonds (see Figure S6).

With the synthetic route to *rac*-**2b** in hand, we focused on the synthesis of optically active **2b**. Initially, we tried to separate the enantiomers of *rac*-**8a** via formation of their (–)–menthol ester. Unfortunately, the two diastereoisomers (**10a** and **10b**, see Scheme 2) were inseparable by flash column chromatography. We then envisaged to resolve the cyclic ketone *rac*-**4** following the procedure employed by Kuehne et al.[22] This led us to obtain the optically pure compounds ($R$,$R_P$)-**2b** and ($S$,$S_P$)-**2b** from ($R_P$)-**4** and ($S_P$)-**4**, respectively, by repeating the same synthetic sequence as that used to synthesize *rac*-**2b** (Scheme 2). The high degree of diastereoselectivity during the Michael addition is crucial for the formation of the enantiopure **2b**. The absolute configuration of the asymmetric centers in ($S$,$S_P$)-**8a** and ($R$,$R_P$)-**8a** was confirmed from their single crystal structures (Figure 4). These configurations were indeed retained in the respective final desired compounds ($S$,$S_P$)-**2b** and ($R$,$R_P$)-**2b**. Interestingly, both the molecules, ($S$,$S_P$)-**8a** and ($R$,$R_P$)-**8a** form infinite chiral 1D helix by intermolecular H-bonding which are mirror images of each other (see Figure S5). The chiral HPLC traces of ($R$,$R_P$)- and ($S$,$S_P$)-**9a** showed $> 99\%$ enantiopurity and the retention times were 16.3 and 24.7 minutes for ($R$,$R_P$)- and ($S$,$S_P$)-**9a**, respectively (see Figure S1, S2, and S3 for the HPLC traces). The CD spectra for both isomers were also recorded and as expected, those of ($R$,$R_P$)- and ($S$,$S_P$)-**2a** were found to be mirror images of each other (see Figure S4).

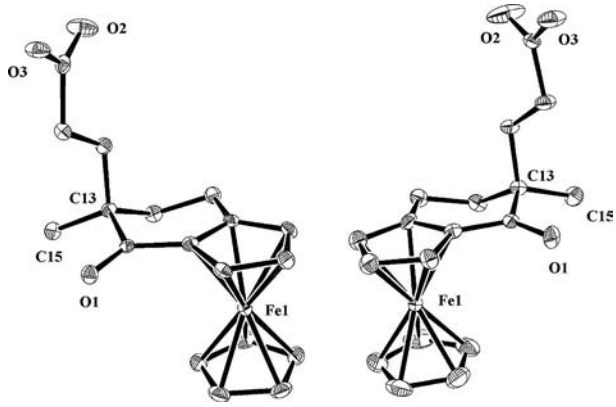


Figure 4. ORTEP plots of enantiopure carboxylic acids ($S$,$S_P$)-**8a** (left) and ($R$,$R_P$)-**8a** (right) (ellipsoids drawn at 50% probability level). Hydrogen atoms are omitted for clarity.

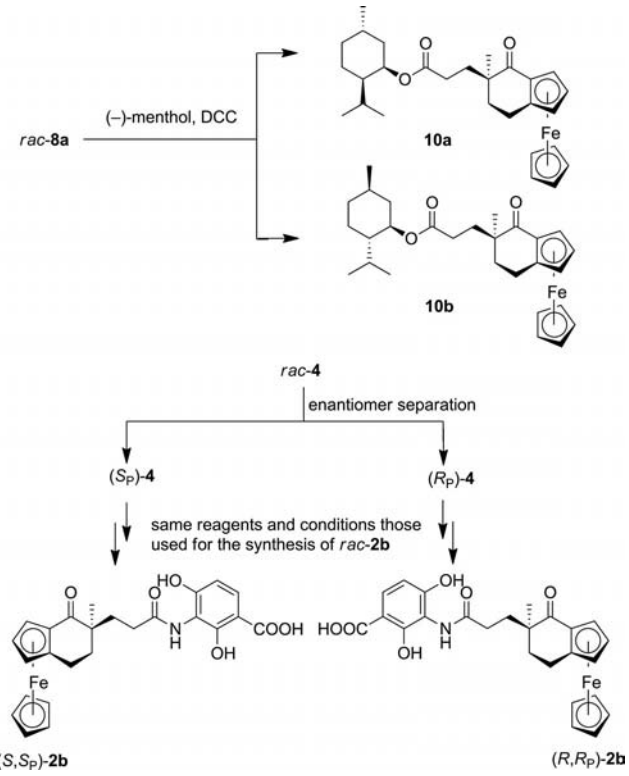


Scheme 2. Synthesis of (–)–menthol esters of *rac*-**8a** (**10a** and **10b**), ($S$,$S_P$)-**2b** and ($R$,$R_P$)-**2b**. ($S_P$)-**4** and ($R_P$)-**4** were prepared from *rac*-**4** following the previously reported procedures.[22]

### Biological Evaluation

One of the very important characteristics of a good antibacterial agent is its low toxicity to mammalian cell lines. The cytoxicity of our new biorganometallics, *rac*-**2b**, ($R$,$R_P$)-**2b** and ($S$,$S_P$)-**2b**, was checked against MCF7, HT29 and Panc1 mammalian cell lines and the test suggested that none of them were active against any of the cell lines up to a concentration of 500 μM (see Supporting Information).

The antimicrobial activities of the new ferrocene-containing bioorganometallics *rac*-**2a**, *rac*-**2b**, ($R$,$R_P$)-**2b** and ($S$,$S_P$)-**2b** were tested against various bacterial strains including Gram-positive methicilline or vancomycin resistant strains [*S. aureus* SG551, *S. aureus* COL (MRSA), *S. aureus* Mu50 (VISA), *S. aureus* ATCC43300 (MRSA)] and Gram-negative (*E. coli* W3110 and *P. aeruginosa* PA01) bacterial strains up to 200 μg/mL. The methyl-protected *rac*-**2a** as well as the completely deprotected *rac*-**2b**, ($R$,$R_P$)-**2b** and ($S$,$S_P$)-**2b** had no antibacterial activity against all tested bacterial strains with concentrations up to 200 μg/mL.

## Conclusions

In this work, we present the first enantiopure metal derivatives of platensimycin. An efficient synthetic route to racemic and optically pure planar chiral ferrocene-containing biorganometallics **2b** inspired by the antibiotic platensimycin lead structure has been developed. This chemistry provides the first examples of C6–C7 substituted platensimycin derivatives for structure-activity studies. The efficient multistep synthetic strategy may set an example for the synthesis of other ferrocene-containing bioorganometallics. The cytotoxicity and antibacterial activity was studied against various mammalian and bacterial cell lines, respectively. Chemically, an important finding of this study is the high stereoselectivity of the Michael addition of 1,2-(α-

  

keto-β-methyltetramethylene)ferrocene (**5a/5b**) to alkyl acrylate esters which has not been investigated before. Furthermore, the absolute configuration of the asymmetric centers generated by the stereoselective Michael addition was confirmed by the determination of the single-crystal structures of ($S$,$S_P$)- and ($R$,$R_P$)-**8a**. Docking experiments with ($S$,$S_P$)-**2b** in the active site of the FabF enzyme revealed the existence of a pocket for bulky cage-like moieties fused to the C6–C7 position of the cyclohexenone unit. This observation can also in principle be useful for designing a completely new class of purely organic analogues of **1a** with C6–C7-fused bulky cages for structure activity relationship (SAR) studies. Unfortunately, none of the enantiomers of **2b** exhibits antibacterial activity up to 200 μg/mL. This lack of activity does not necessarily devaluate other C6–C7-fused platensimycin derivatives. It may perhaps simply be due to the poor cellular uptake of our compounds as demonstrated for several other synthetic and natural congeners of **1a** having a modified tetracyclic cage.[4h] We are currently synthesizing other C6–C7 organometallic fused analogues of **2b** using this multistep synthetic route to examine this design further in terms of SAR studies. These results will be published in due course.

## Experimental Section

**Materials:** All chemicals were of reagent grade quality or better, obtained from commercial suppliers and used without further purification. Solvents were used as received or dried with molecular sieves. All preparations were carried out using standard Schlenk techniques. *rac*-**4** was prepared from commercially available 4-ferrocenyl-4-oxobutyric acid via 4-ferrocenylbutyric acid[24] following slightly modified literature procedure.[20,25] (+)-(*S*)-*N*,*S*-Dimethyl-*S*-phenylsulfoximine was prepared from (+)-(*S*)-*S*-methyl-*S*-phenylsulfoximine and used for the preparation of optically active ($R_P$)-**4** and ($S_P$)-**4** from *rac*-**4** following the procedure reported earlier.[22,26] Methyl 3-amino-2,4-dimethoxybenzoate was prepared from methyl 3-nitro-2,4-dihydroxybenzoate[27] by methyl protection (with 9 equiv. $K_2CO_3$, 8 equiv. MeI in $CH_3CN$) and subsequent reduction of the nitro group following the procedure described by McNulty and co-workers.[23]

**Instrumentation and Methods:** $^1H$ and $^{13}C$ NMR spectra were recorded in deuterated solvents on Bruker DRX 200, 250, 400, or 600 spectrometers at 30 °C. The chemical shifts, $\delta$, are reported in ppm (parts per million). The residual solvent peaks have been used as an internal reference. The abbreviations for the peak multiplicities are as follows: s (singlet), d (doublet), dd (doublet of doublets), t (triplet), q (quartet), m (multiplet), and br (broad). Infrared spectra were recorded on an ATR unit using a Bruker Tensor 27 FTIR spectrophotometer at 4 $cm^{-1}$ resolution. Signal intensities: s (strong), m (medium), w (weak), and br. (broad). ESI mass spectra were recorded on a Bruker Esquire 6000. Crystallographic data for *rac*-**5a**, *rac*-**6a**, *rac*-**8a**, ($S$,$S_P$)-**8a** and ($R$,$R_P$)-**8a** and *rac*-**2b** were collected using a Bruker-axs SMART 1000 CCD diffractometer. The structure was solved by direct methods (SHELXS-97[28]) and refined against $F^2$ with all measured reflections (SHELXL-97,[28] Palton–Squeeze[29]). Elemental microanalyses were performed using a Fisons Carlo–Erba EA1108 instrument (CHNS version). The enatiopurities of **9a** was checked by HPLC using a Daicel Chiralpak-IA HPLC column (250 × 4.6 mm) on a KNAUER HPLC System. The flow rate was 1 mL/min and UV absorption was measured at 254 nm. An isocratic condition of 40/60 2-propanol/hexanes was applied. CD spectra were recorded on a JASCO J-810 CD spectrometer (220 to 350 and 300 to 600 nm scanning speed of 50 nm/min, accumulation of 8 scans). The manual docking of ($S$,$S_P$)-**2b** with FabF was done using PyMOL (PyMOL-1_2edu-bin-win32).

### Biology

**Cell Culture and Cytotoxicity Test:** MCF7, HT29 and Panc1 cells were cultured in RPMI 1640 medium supplemented with 10% fetal calf serum (FCS), 2 mM L-glutamine, penicillin (100 U/mL) and streptomycin (100 mg/mL) in a 5% $CO_2$ atmosphere. In vitro cytotoxicity of the compounds was studied on MCF7, HT29 and Panc1 cells. Cell viability, which correlates with the metabolic activity of a cell, was determined by the resazurin assay. In addition to the cell viability, absolute cell numbers were determined by the crystal violet assay, which can be applied after elution of resazurin. Both the assay shows similar results, if compounds are not toxic to the maintained cell lines. Cells were seeded in 96-well cell-culture treated microtiter plates (MTP). After seeding, the cells were grown for 24 h under standard conditions. The compounds were dissolved in culture medium with 0.5% DMSO and applied to the cells in 1, 5, 20, 50, 100 and 500 μM concentrations for 48 h. Before resazurin was added to the cells, they were washed three times with Phenol-Red-free RPMI 1640 medium. A 10% solution of resazurin (v/v) in Phenol-Red-free RPMI 1640 medium was added. Absorbance at 600 nm was directly measured on a Tecan Sapphire 2 microplate reader (Tecan, Germany) at 378 °C. After 2 h of incubation at 378 °C and 5% $CO_2$, the measurement was repeated. The decrease in absorbance gave the viability. Resazurin was removed and the cells were fixed with 4% paraformaldehyde (PFA) in phosphate buffered saline (PBS) for 15 min at room temperature. PFA was eluted two times with PBS and membranes were permeabilized by Triton X-100 (0.1%) in PBS for 10 min. Afterwards, aq. crystal violet solution (0.04%) was added to the cells and the MTP was mechanically shaken for 1 h. The cells were washed with $H_2O$ (× 7), and crystal violet was eluted with 70% EtOH for 3.5 h. The absorbance was determined at 570 nm, cell biomass could be calculated after subtraction of 24 h pre-substance incubation absorbance values. The obtained viability or cytotoxicity data were plotted against the concentration with Origin 8 (Originlab, Northampton, USA).

**Minimum Inhibitory Concentration (MIC) Determination:** Minimun inhibitory concentrations (MICs) against all bacterial strains were determined in a microtiter plate assay containing 0.2 mL of Luria Broth medium and appropriate compound concentrations up to 200 μg/mL. The tubes were inoculated with $10^5$ cells/mL and incubated at 37 °C for 18 h. The MIC was defined as the lowest concentration that inhibited visible growth.

### Synthesis

**Mixture of *rac*-5a and *rac*-5b:**[30] To a stirred solution of *rac*-**4** (200 mg, 0.79 mmol) in 10 mL of THF, 0.5 M KHMDS in toluene (2.38 mL, 1.19 mmol) was added slowly at –78 °C. The mixture was allowed to stir for 30 min, HMPA (1.6 mL) and MeI (897 mg, 6.32 mmol) was then added sequentially. After 3 h at –78 °C, the reaction was quenched with saturated $NaHCO_3$ solution and extracted with $Et_2O$ (3 × 30 mL). The organic phase was washed with $H_2O$, brine, dried with anhydrous $Na_2SO_4$, filtered and concentrated. Flash column chromatography (silica gel, hexane/EtOAc, 4:1) gave a mixture of *rac*-**5a** (≈ 90%) and *rac*-**5b** (≈ 10%) as red solid (160 mg, 76%). Pure *rac*-**5a** can be obtained by a single recrystallization from pentane.

  

**Data for *rac*-5a:** $R_f$ = 0.37 (silica gel, hexane/EtOAc, 4:1). $^1$H NMR (400 MHz, $CDCl_3$): $\delta$ = 1.14 (d, 3 H, C$H_3$), 1.74–1.83 (m, 1 H, cyclohexenone), 2.29–2.37 (m, 1 H, cyclohexenone), 2.50–2.60 (m, 1 H, cyclohexenone), 2.62–2.76 (m, 2 H, cyclohexenone), 4.14 (s, 5 H, $C_5H_5$), 4.43 (m, 1 H, $C_5H_3$), 4.48 (m, 1 H, $C_5H_3$), 4.80 (m, 1 H, $C_5H_3$) ppm. $^{13}$C NMR (400 MHz, $CDCl_3$): $\delta$ = 15.7, 21.1, 31.1, 41.8, 65.3, 70.1, 70.4, 70.5, 74.4, 91.9, 207.5 ppm. IR: $\tilde{\nu}$ = 3078 (w), 2956 (w), 2932 (w), 1658 (s), 1464 (m), 1440 (m), 1370 (m), 1336 (m), 1277 (w), 1141 (w), 1075 (m), 1021 (m), 953 (w), 927 (w), 891 (w), 855 (m), 830 (m), 760 (w), 620 (w) cm$^{-1}$. ESI-MS (pos. detection mode): *m*/*z* (%) = 301.07 (35) $[M + MeOH + H]^+$, 291.03 (100) $[M + Na]^+$, 269.06 (27) $[M + H]^+$. $C_{15}H_{16}FeO$ (268.14): calcd. C 67.19, H 6.01; found C 67.18, H 6.09.

**Michael Addition of Methyl Acrylate to the Mixture of *rac*-5a and *rac*-5b to Give a Mixture of *rac*-6a and *rac*-6b:** To a stirred solution of the mixture of *rac*-**5a** and *rac*-**5b** (700 mg, 2.61 mmol) in 14 mL of *t*BuOH and $Et_2O$ (1:1) mixture, KO*t*Bu (585 mg, 5.22 mmol) was added at 0 °C. After 15 min, methyl acrylate (2.25 mg, 26.12 mmol) was added to the reaction mixture and allowed to stir for 2.5 h at 0 °C. The reaction was quenched with saturated $NH_4Cl$ solution and the aqueous layer was extracted with EtOAc (2 × 40 mL). The organic layer was washed with $H_2O$, brine, dried with anhydrous $Na_2SO_4$, filtered and concentrated. Flash column chromatography (silica gel, hexane/EtOAc, 6:1) gave a mixture of *rac*-**6a** (≈ 90%) and *rac*-**6b** (≈ 10%) as red sticky solid (560 mg, 61%). Pure *rac*-**6a** can be obtained by recrystallization from a diethyl ether/pentane solution of *rac*-**6a** and *rac*-**6b**.

**Data for *rac*-6a:** $R_f$ = 0.29 (silica gel, hexane/EtOAc, 4:1). $^1$H NMR (400 MHz, $CDCl_3$): $\delta$ = 1.23 (s, 3 H, C$H_3$), 1.58–1.68 (m, 1 H, cyclohexenone), 1.78–1.92 (m, 2 H, C$H_2$-$CH_2$-$COOCH_3$), 2.15–2.21 (m, 1 H, cyclohexenone), 2.26–2.36 (m, 2 H, cyclohexenone), 2.51–2.59 (m, 2 H, $CH_2$-C$H_2$-$COOCH_3$), 3.60 (s, 3 H, -OC$H_3$), 4.15 (s, 5 H, $C_5H_5$), 4.42–4.46 (m, 2 H, $C_5H_3$), 4.81–4.83 (m, 1 H, $C_5H_3$) ppm. $^{13}$C NMR (400 MHz, $CDCl_3$): $\delta$ = 20.4, 21.7, 28.7, 30.3, 36.5, 45.3, 51.3, 66.4, 69.8, 70.1, 70.9, 74.1, 90.8, 173.7, 207.7 ppm. IR: $\tilde{\nu}$ = 2930 (w), 1733 (s), 1662 (s), 1435 (s), 1372 (m), 1351 (w), 1331 (w), 1296 (s), 1270 (m), 1195 (s), 1174 (s), 1106 (m), 1032 (w), 1001 (w), 943 (w), 820 (s), 770 (w), 729 (s), 649 (w) cm$^{-1}$. ESI-MS (pos. detection mode): *m*/*z* (%) = 354.07 (100) $[M]^+$. $C_{19}H_{22}FeO_3$ (354.23): calcd. C 64.42, H 6.26; found C 64.56, H 6.22.

**Michael Addition of *tert*-Butyl Acrylate to the Mixture of *rac*-5a and *rac*-5b to Give *rac*-7a:** To a stirred solution of a mixture of *rac*-**5a** and *rac*-**5b** (100 mg, 0.37 mmol) in 4 mL of *t*BuOH and $Et_2O$ (1:1) mixture, KO*t*Bu (83 mg, 0.74 mmol) was added at 0 °C. After 15 min, *tert*-butyl acrylate (710 mg, 5.55 mmol) was added to the reaction mixture and allowed to stir for 5 h at 0 °C. The reaction was quenched with saturated $NH_4Cl$ and the aqueous layer was extracted with EtOAc (2 × 15 mL). The organic layer was washed with $H_2O$, brine, dried with anhydrous $Na_2SO_4$, filtered. The solvent and excess *tert*-butyl acrylate was removed using high vacuum pump. Flash column chromatography (silica gel, hexane/EtOAc, 8:1) gave *rac*-**7a** as orange crystalline solid (120 mg, 81%).

**Data for *rac*-7a:** $R_f$ = 0.17 (silica gel, hexane/EtOAc, 6:1). $^1$H NMR (400 MHz, $CDCl_3$): $\delta$ = 1.22 (s, 3 H, C$H_3$), 1.37 [s, 9 H, -C(C$H_3$)$_3$], 1.53–1.63 (m, 1 H, cyclohexenone), 1.71–1.82 [m, 1 H, C$H_2$-$CH_2$-COOC(C$H_3$)$_3$], 1.85–1.92 [m, 1 H, C$H_2$-$CH_2$-COOC-(C$H_3$)$_3$], 2.03–2.34 (m, 3 H, cyclohexenone), 2.50–2.55 [m, 2 H, $CH_2$-C$H_2$-COOC(C$H_3$)$_3$], 4.15 (s, 5 H, $C_5H_5$), 4.42–4.46 (m, 2 H, $C_5H_3$), 4.81–4.83 (m, 1 H, $C_5H_3$) ppm. $^{13}$C NMR (400 MHz, $CDCl_3$): $\delta$ = 20.4, 21.7, 28.7, 30.2, 30.3, 36.5, 45.3, 66.4, 69.8, 70.1, 70.9, 74.1, 80.1 90.8, 173.7, 207.7 ppm. IR: $\tilde{\nu}$ = 2930 (w), 1719 (s), 1660 (s), 1465 (m), 1435 (m), 1365 (w), 1349 (w), 1330 (w), 1270 (m), 1154 (w), 1137 (s), 1117 (s), 1106 (m), 1032 (w), 1001 (w), 943 (w), 844 (s), 826 (s), 770 (w), 729 (s), 649 (w) cm$^{-1}$. ESI-MS (pos. detection mode): *m*/*z* (%) = 395.98 (100) $[M]^+$, 418.94 (15) $[M + Na]^+$. $C_{22}H_{28}FeO_3$ (396.31): calcd. C 66.68, H 7.12; found C 66.63, H 7.23.

**Carboxylic Acid *rac*-8a. General Procedure:** To a stirred solution of the Me or *t*Bu ester in THF/MeOH, 1 M aqueous NaOH was added and the mixture was stirred 16 h at room temperature. The reaction mixture was then acidified with 1 M HCl up to ca. pH 2 and extracted with EtOAc. The combined organic phase was washed with $H_2O$, brine, dried with anhydrous $Na_2SO_4$, filtered and concentrated. The carboxylic acid *rac*-**8a** was obtained as red solid.

**From *rac*-6a:** *rac*-**6a** (300 mg, 0.84 mmol), THF (10 mL), 1 M aqueous NaOH (10 mL); yield of *rac*-**8a** is 270 mg, 93%.

**From the Mixture of *rac*-6a and *rac*-6b:** (300 mg, 0.84 mmol), THF (10 mL), 1 M aqueous NaOH (10 mL). The red solid obtained was recrystalized from $CHCl_3$/EtOAc mixture at 0 °C to yield red crystals of pure *rac*-**8a** which was collected and washed with cold $CHCl_3$ or $Et_2O$; yield of *rac*-**8a** is 217 mg, 70%.

**From *rac*-7a:** *rac*-**7a** (114 mg, 0.28 mmol), 1:1 THF/MeOH (6 mL), 1 M aqueous NaOH (3.5 mL); yield of *rac*-**8a** is 89 mg, 91%.

**Data for *rac*-8a:** $R_f$ = 0.60 (silica gel, EtOAc). $^1$H NMR (400 MHz, $CDCl_3$): $\delta$ = 1.23 (s, 3 H, C$H_3$), 1.55–1.67 (m, 1 H, cyclohexenone), 1.75–1.89 (m, 2 H, C$H_2$-$CH_2$-COOH), 2.16–2.23 (m, 1 H, cyclohexenone), 2.27–2.42 (m, 2 H, cyclohexenone), 2.46–2.61 (m, 2 H, $CH_2$-C$H_2$-COOH), 4.15 (s, 5 H, $C_5H_5$), 4.41–4.49 (m, 2 H, $C_5H_3$), 4.75–4.85 (m, 1 H, $C_5H_3$) ppm. $^{13}$C NMR (400 MHz, $CDCl_3$): $\delta$ = 20.4, 21.6, 28.8, 30.1, 36.8, 45.1, 66.4, 69.8, 70.1, 70.9, 74.1, 90.8, 178.7, 208.7 ppm. IR: $\tilde{\nu}$ = 3103 (w), 2931 (m), 1715 (s), 1626 (s), 1467 (m), 1420 (m), 1406 (w), 1375 (w), 1356 (w), 1331 (w), 1279 (m), 1257 (s), 1197 (s), 1163 (m), 1106 (w), 947 (w), 822 (s), 690 (m), 626 (m) cm$^{-1}$. ESI-MS (neg. detection mode): *m*/*z* (%) = 338.96 (100) $[M - H]^-$. $C_{18}H_{20}FeO_3 \cdot 0.25H_2O$ (344.69): calcd. C 62.66, H 6.01; found C 62.70, H 6.21.

**(–)–Menthol Esters of *rac*-8a (10a and 10b):** To a stirred solution of the carboxylic acid *rac*-**8a** (200 mg, 0.59 mmol) in 20 mL of $CH_2Cl_2$, dicyclohexylcarbodiimide (DCC) (146 mg, 0.71 mmol), 4-(dimethylamino)pyridine (DMAP) (7.2 mg, 0.06 mmol) and (–)-menthol (138 mg, 0.89 mmol) were added and the mixture was allowed to stir for 6 h at room temperature under an argon atmosphere. The reaction mixture was diluted with 30 mL of $CH_2Cl_2$ and washed several times with water and brine (1 × 30 mL). The organic phase was dried with anhydrous $Na_2SO_4$, filtered and concentrated. Flash column chromatography (silica gel, hexane/EtOAc, 7:1) gave a 1:1 mixture of **10a** and **10b** as red liquid (191 mg, 68%).

**Data for 1:1 Mixture of 10a and 10b:** $R_f$ = 0.56 (silica gel, hexane/EtOAc, 3.5:1). $^1$H NMR (400 MHz, $CDCl_3$): $\delta$ = 0.65–0.72 (m, 3 H), 0.77–1.03 (m, 9 H), 1.22 (s, 3 H) 1.24–1.33 (m, 1 H), 1.36–1.45 (m, 1 H), 1.56–1.67 (m, 3 H), 1.72–1.82 (m, 2 H), 1.85–1.92 (m, 2 H), 2.09–2.19 (m, 1 H), 2.23–2.34 (m, 2 H), 2.49–2.54 (m, 2 H), 4.12 (s, 5 H) 4.40–4.44 (m, 2 H), 4.55–4.62 (m, 1 H) 4.78–4.82 (m, 1 H) ppm. $^{13}$C NMR (400 MHz, $CDCl_3$): $\delta$ = 16.2 and 16.3, 20.4, 20.7, 21.7 and 21.8, 21.9 and 22.0, 23.3 and 23.4, 26.1 and 26.2, 29.4 and 29.5, 30.2 and 30.3, 31.2, 34.2, 36.6 and 36.7, 40.8 and 40.9, 45.1, 46.9, 66.2, 69.5, 70.1, 70.8, 74.0 and 74.1, 74.2 and 74.3, 90.9 and 91.0, 173.0 and 173.1, 207.7 and 207.8 ppm. IR: $\tilde{\nu}$ = 2927 (m), 2867 (m), 1726 (s), 1666 (s), 1437 [m (br.)], 1371 (w), 1332 (w), 1294 (w), 1176 (s), 1106 (w), 983 (w), 819 (w) cm$^{-1}$. ESI-MS (pos. detection mode): *m*/*z* (%) = 478.07 (100) $[M]^+$.

  

**Amide *rac*-9a:** To a stirred solution of the carboxylic acid *rac*-**8a** (100 mg, 0.29 mmol) in 3 mL of DMF, HATU (220 mg, 0.58 mmol) and DIPEA (72 mg, 0.58 mmol) were added and the mixture was allowed to stir for 30 min under an argon atmosphere. Methyl 3-amino-2,4-dimethoxybenzoate (124 mg, 0.58 mmol) in 3 mL of acetonitrile was then added and the mixture was stirred for 65 h at room temperature. The reaction mixture was diluted with 30 mL of EtOAc and washed with $H_2O$ and brine. The organic phase was dried with anhydrous $Na_2SO_4$, filtered and concentrated. Flash column chromatography (silica gel, hexane/EtOAc, 1:1→0:1) gave *rac*-**9a** as red sticky solid. Co-evaporation of the sticky solid with $Et_2O$ afforded orange color powder (140 mg, 89%).

**Data for *rac*-9a:** $R_f$ = 0.50 (silica gel, EtOAc). $^1$H NMR (400 MHz, $CDCl_3$): $\delta$ = 1.25 (s, 3 H, C$H_3$), 1.73–1.83 (m, 1 H, cyclohexenone), 1.87–1.98 (m, 2 H, C$H_2$-$CH_2$-CONH), 2.16–2.27 (m, 1 H, cyclohexenone), 2.30–2.42 (m, 2 H, cyclohexenone), 2.49–2.62 (m, 2 H, $CH_2$-C$H_2$-CONH), 3.73 (s, 3 H, COOC$H_3$), 3.82 (s, 3 H, OC$H_3$), 3.87 (s, 3 H, OC$H_3$), 4.16 (s, 5 H, $C_5H_5$), 4.42–4.48 (m, 2 H, $C_5H_3$), 4.78–4.83 (m, 1 H, $C_5H_3$), 6.61 (br. s, 1 H, N*H*), 6.68 (d, 1 H, phenyl H), 7.81 (d, 1 H, phenyl H) ppm. $^{13}$C NMR (400 MHz, $CDCl_3$): $\delta$ = 20.4, 21.7, 30.8, 30.9, 37.1, 45.1, 51.9, 56.1, 61.9, 66.1, 69.9, 70.1, 70.9, 74.1, 91.1, 106.6, 116.9, 120.3, 131.7, 157.7, 159.1, 165.9, 172.3, 208.7 ppm. IR: $\tilde{\nu}$ = 3256 (w), 2933 (w), 1721 (m), 1660 (s), 1594 (m), 1464 (m), 1443 (s), 1414 (m), 1373 (w), 1351 (w), 1270 (s), 1217 (w), 1185 (w), 1140 (w), 1097 (s), 1004 (m), 941 (m), 821 (w), 789 (m), 751 (m), 680 (w) cm$^{-1}$. ESI-MS (pos. detection mode): *m*/*z* (%) = 533.08 (100) $[M]^+$, 556.03 (90) $[M + Na]^+$.

**Compounds *rac*-2a and *rac*-2b:** To a stirred solution of the amide *rac*-**9a** (250 mg, 0.47 mmol) in 3 mL of $CHCl_3$, $BBr_3$ (0.45 mL, 4.69 mmol) was added at about –78 °C (just before the solution freezes) under $N_2$ atmosphere. The mixture turned blue immediately and stirred 20 h at room temperature. The reaction mixture was poured in to 20 mL of distilled water, stirred further 30 min and extracted with EtOAc (3× 25 mL). The organic phase was washed with brine (40 mL), dried with anhydrous $Na_2SO_4$, filtered and concentrated. Flash column chromatography on silica gel (pure EtOAc→EtOAc/MeOH/AcOH, 20:1:0.1) gave *rac*-**2a** (85 mg, orange solid), followed by *rac*-**2b** (81 mg, orange solid).

A solution of *rac*-**2a** (85 mg, 0.168 mmol) in 8 mL of 1:3 mixture of THF and MeOH, 1 M NaOH solution (7.2 mL) was added. The mixture was deoxygenated by $N_2$ bubbling for 15 min and heated at 60 °C for 16 h. The reaction mixture was diluted with 50 mL of distilled water, acidified with 1 M HCl up to pH ≈ 2 and extracted with EtOAc. The organic phase was dried with anhydrous $Na_2SO_4$, filtered and concentrated. Flash column chromatography (silica gel, EtOAc/MeOH/AcOH, 20:1:0.1) afforded *rac*-**2b** (74 mg) as orange color solid. Combined yield of *rac*-**2b** (155 mg, 79%).

**Data for *rac*-2a:** $R_f$ = 0.82 (silica gel, EtOAc/MeOH/AcOH, 20:1:0.1). $^1$H NMR (400 MHz, $CDCl_3$): $\delta$ = 1.31 (s, 3 H, C$H_3$), 1.64–1.83 (m, 1 H, cyclohexenone), 1.87–2.10 (m, 2 H, C$H_2$-$CH_2$-CONH), 2.27–2.47 (m, 2 H, cyclohexenone), 2.50–2.67 (m, 3 H, $CH_2$-C$H_2$-CONH and cyclohexenone), 3.91 (s, 3 H, COOC$H_3$), 4.15 (s, 5 H, $C_5H_5$), 4.42–4.48 (m, 2 H, $C_5H_3$), 4.78–4.83 (m, 1 H, $C_5H_3$), 6.46 (d, 1 H, phenyl H), 6.51 (d, 1 H, phenyl H), 7.90 (br. s, 1 H, N*H*), 10.95 (br. s, 1 H, O*H*), 11.62 (br. s, 1 H, O*H*) ppm. $^{13}$C NMR (400 MHz, $CDCl_3$): $\delta$ = 20.5, 21.8, 30.9, 31.4, 37.2, 45.3, 52.2, 66.3, 69.9, 70.3, 70.9, 74.1, 90.9, 104.3, 111.1, 114.3, 127.3, 153.7, 154.9, 170.9, 173.3, 208.2 ppm. IR: $\tilde{\nu}$ = 2926 (w), 2582 (w), 1651 [s (br)], 1595 (s), 1532 (s), 1467 (w), 1437 (s), 1375 (m), 1339 (s), 1292 (m), 1216 (s), 1145 (m), 1032 (w), 952 (w), 897 (w), 787 (s), 682 (w) cm$^{-1}$. ESI-MS (pos. detection mode): *m*/*z* (%) = 505.08 (100) $[M]^+$, 528.04 (50) $[M + Na]^+$.

**Data for *rac*-2b:** $R_f$ = 0.21 (silica gel, EtOAc/MeOH/AcOH, 20:1:0.1). $^1$H NMR (400 MHz, $CDCl_3$): $\delta$ = 1.33 (s, 3 H, C$H_3$), 1.73–1.87 (m, 1 H, cyclohexenone), 1.92–2.12 (m, 2 H, C$H_2$-$CH_2$-CONH), 2.36–2.48 (m, 2 H, cyclohexenone), 2.50–2.69 (m, 3 H, $CH_2$-C$H_2$-CONH and cyclohexenone), 4.17 (s, 5 H, $C_5H_5$), 4.42–4.50 (m, 2 H, $C_5H_3$), 4.79–4.89 (m, 1 H, $C_5H_3$), 6.51 (br. d, 1 H, phenyl H), 7.68 (br. s, 1 H, N*H*), 8.11 (br. d, 1 H, phenyl H) ppm. $^{13}$C NMR (400 MHz, $CDCl_3$): $\delta$ = 20.6, 21.7, 30.7, 31.2, 36.1, 45.3, 65.9, 69.9, 70.3, 70.9, 74.3, 91.1, 105.7, 108.1, 113.3, 129.3, 159.1, 159.7, 172.3, 172.5, 207.7 ppm. IR: $\tilde{\nu}$ = 2925 (w), 1713 (m), 1649 (s), 1603 (s), 1533 (s), 1400 (m), 1314 (w), 1279 (s), 1244 (s), 1217 (s), 1154 (m), 1059 (w), 981 (w), 790 (s), 681 (w) cm$^{-1}$. ESI-MS (neg. detection mode): *m*/*z* (%) = 489.96 (100) $[M - H]^-$.

Table 1. Selected crystallographic data and parameters for *rac*-**2b**, *rac*-**5a**, *rac*-**6a**, *rac*-**8a**, ($S$,$S_P$)-**8a**, ($R$,$R_P$)-**8a**.

| | *rac*-**2b** | *rac*-**5a** | *rac*-**6a** | *rac*-**8a** | ($S$,$S_P$)-**8a** | ($R$,$R_P$)-**8a** |
|---|---|---|---|---|---|---|
| CCDC | 791976 | 791973 | 791972 | 791971 | 791974 | 791975 |
| Empirical formula | $C_{25}H_{25}FeNO_6$ | $C_{15}H_{16}FeO$ | $C_{19}H_{22}FeO_3$ | $C_{18}H_{20}Fe\ O_3$ | $C_{18}H_{20}FeO_3$ | $C_{18}H_{20}FeO_3$ |
| FW | 491.31 | 268.13 | 354.22 | 340.19 | 340.19 | 340.19 |
| Temperature /K | 173 | 223 | 223 | 223 | 203 | 223 |
| Crystal system | triclinic | triclinic | triclinic | monoclinic | monoclinic | monoclinic |
| Space group | $P\bar{1}$ | $P\bar{1}$ | $P\bar{1}$ | $P2_1/c$ | $P2_1$ | $P2_1$ |
| *a* /Å | 8.625(10) | 6.608(3) | 6.7528(14) | 9.422(4) | 7.8994(3) | 7.913(18) |
| *b* /Å | 12.320(13) | 8.833(4) | 11.632(2) | 10.315(5) | 11.4853(3) | 11.55(2) |
| *c* /Å | 12.352(13) | 11.436(5) | 12.018(2) | 16.426(6) | 9.2746(4) | 9.33(2) |
| $\alpha$ | 91.726(17) | 69.933(8) | 117.25(3) | 90 | 90 | 90 |
| $\beta$ | 92.428(9) | 78.573(9) | 96.47(3) | 107.07(2) | 115.163(5) | 114.42(9) |
| $\gamma$ | 101.620(14) | 73.539(8) | 90.20(3) | 90 | 90 | 90 |
| *V* /Å$^3$ | 1283(2) | 597.5(5) | 832.3(3) | 1526.1(11) | 761.60(5) | 776(3) |
| Z | 2 | 2 | 2 | 4 | 2 | 2 |
| $D_{calc}$ /mg m$^{-3}$ | 1.271 | 1.490 | 1.413 | 1.481 | 1.483 | 1.455 |
| $\mu$ /mm$^{-1}$ | 0.625 | 1.240 | 0.918 | 0.998 | 1.000 | 0.981 |
| *F*(000) | 512 | 280 | 372 | 712 | 356 | 356 |
| Reflections collected | 11084 | 3293 | 4543 | 2651 | 8634 | 4076 |
| Independent reflections | 4501 | 2063 | 2842 | 2653 | 2678 | 2139 |
| *R*(int) | 0.1029 | 0.0457 | 0.0547 | 0.000 | 0.0262 | 0.0511 |
| GOF on $F^2$ | 1.076 | 1.115 | 0.984 | 1.099 | 0.929 | 0.0437 |
| Final *R* indices (*R*1) [$I > 2\sigma(I)$] | 0.0699 | 0.0609 | 0.0572 | 0.0721 | 0.0227 | 0.1171 |

  

$C_{25}H_{25}FeNO_6 \cdot H_2O$ (509.31): calcd. C 58.95, H 5.34, N 2.75; found C 59.18, H 5.09, N 2.53.

Crystallographic data and CCDC numbers given in Table 1 contain the supplementary crystallographic data for this paper. These data can be obtained free of charge from The Cambridge Crystallographic Data Centre via www.ccdc.cam.ac.uk/data_request/cif.

**Supporting Information** (see footnote on the first page of this article): $^1H$ and $^{13}C$ NMR spectra for the new compounds. Chiral HPLC traces of *rac*-**9a**, (*R*,$R_P$)-**9a**, (*S*,$S_P$)-**9a** and CD spectra of (*R*,$R_P$)-**2b**, (*S*,$S_P$)-**2b**. ORTEP plots of *rac*-**5a**, *rac*-**6a** and *rac*-**8a**. H-bonding interactions in the single crystal structures of (*R*,$R_P$)-**8a**, (*S*,$S_P$)-**8a** and *rac*-**2b**. Results of the cytotoxicity test.

## Acknowledgments

We wish to acknowledge the International Max Plank Research School for Chemical Biology (fellowship to M. P.) and the Deutsche Forschungsgemeinschaft (DFG) (FOR 630) for financial support of this project. Support from the Research Department Interfacial System Chemistry (J. E. B. and N. M.-N.) and funding for both groups from the State of North Rhine-Westphalia (NRW), Germany and the EUROPEAN UNION, European Regional Development Fund, "Investing in your future" is also gratefully acknowledged. G. G. thanks the Swiss National Science Foundation (Ambizione Fellowship, grant number PZ00P2_126404) and the Alexander von Humboldt Foundation for funding as well as Prof. Roger Alberto for generous access to all the facilities of the Institute of Inorganic Chemistry of the University of Zürich. We thank Annegret Knüfer for the cytotoxicity test.

[1] J. Wang, S. M. Soisson, K. Young, W. Shoop, S. Kodali, A. Galgoci, R. Painter, G. Parthasarathy, Y. S. Tang, R. Cummings, S. Ha, K. Dorso, M. Motyl, H. Jayasuriya, J. Ondeyka, K. Herath, C. Zhang, L. Hernandez, J. Allocco, A. Basilio, J. R. Tormo, O. Genilloud, F. Vicente, F. Pelaez, L. Colwell, S. H. Lee, B. Michael, T. Felcetto, C. Gill, L. L. Silver, J. D. Hermes, K. Bartizal, J. Barrett, D. Schmatz, J. W. Becker, D. Cully, S. B. Singh, *Nature* **2006**, *441*, 358–361.

[2] J. Wang, S. Kodali, S. H. Lee, A. Galgoci, R. Painter, K. Dorso, F. Racine, M. Motyl, L. Hernandez, E. Tinney, S. L. Colletti, K. Herath, R. Cummings, O. Salazar, I. Gonzalez, A. Basilio, F. Vicente, O. Genilloud, F. Pelaez, H. Jayasuriya, K. Young, D. F. Cully, S. B. Singh, *Proc. Natl. Acad. Sci. USA* **2007**, *104*, 7612–7616.

[3] D. T. Manallack, I. T. Crosby, Y. Khakham, B. Capuano, *Current Medicinal Chem.* **2008**, *15*, 705–710.

[4] a) K. Tiefenbacher, J. Mulzer, *Angew. Chem.* **2008**, *120*, 6294; *Angew. Chem. Int. Ed.* **2008**, *47*, 6199–6200; b) K. C. Nicolaou, A. Li, D. J. Edmonds, *Angew. Chem.* **2006**, *118*, 7244; *Angew. Chem. Int. Ed.* **2006**, *45*, 7086–7090; c) K. C. Nicolaou, T. Lister, R. M. Denton, A. Montero, D. J. Edmonds, *Angew. Chem.* **2007**, *119*, 4796; *Angew. Chem. Int. Ed.* **2007**, *46*, 4712–4714; d) K. C. Nicolaou, G. S. Tria, D. J. Edmonds, *Angew. Chem.* **2008**, *120*, 1804; *Angew. Chem. Int. Ed.* **2008**, *47*, 1780–1783; e) K. C. Nicolaou, Y. Tang, J. Wang, A. F. Stepan, A. Li, A. Montero, *J. Am. Chem. Soc.* **2007**, *129*, 14850–14851; f) O. V. Barykina, K. L. Rossi, M. J. Rybak, B. B. Snider, *Org. Lett.* **2009**, *11*, 5334–5337; g) K. Palanichamy, K. P. Kaliappan, *Chem. Asian J.* **2010**, *5*, 668–703; h) C. Zhang, J. Ondeyka, K. Herath, H. Jayasuriya, Z. Guan, D. L. Zink, L. Dietrich, B. Burgess, S. N. Ha, J. Wang, S. B. Singh, *J. Nat. Prod.* **2010**, *74*, 329–340.

[5] S. B. Singh, H. Jayasuriya, K. B. Herath, C. Zhang, J. G. Ondeyka, D. L. Zink, S. Ha, G. Parthasarathy, J. W. Becker, J. Wang, S. M. Soisson, *Tetrahedron Lett.* **2009**, *50*, 5182–5185.

[6] C. Zhang, J. Ondeyka, D. L. Zink, B. Burgess, J. Wang, S. B. Singh, *Chem. Commun.* **2008**, 5034–5036.

[7] a) K. C. Nicolaou, A. F. Stepan, T. Lister, A. Li, A. Montero, G. S. Tria, C. I. Turner, Y. Tang, J. Wang, R. M. Denton, D. J. Edmonds, *J. Am. Chem. Soc.* **2008**, *130*, 13110–13119; b) K. Tiefenbacher, A. Gollner, J. Mulzer, *Chem. Eur. J.* **2010**, *16*, 9616–9622.

[8] K. P. Jang, C. H. Kim, S. W. Na, H. Kim, H. Kang, E. Lee, *Bioorg. Med. Chem. Lett.* **2009**, *19*, 4601–4602.

[9] M. Patra, G. Gasser, A. Pinto, K. Merz, I. Ott, J. E. Bandow, N. Metzler-Nolte, *ChemMedChem* **2009**, *4*, 1930–1938.

[10] M. Wenzel, M. Patra, D. Albrecht, D. Y.-K. Chen, K. C. Nicolaou, N. Metzler-Nolte, J. E. Bandow, *Antimicrob. Agents Chemother.* **2011**, *55*, 2590–2596.

[11] S. Brinster, B. Lamberet, B. Staels, P. Trieu-Cuot, A. Gruss, C. Poyart, *Nature* **2009**, *458*, 83–86.

[12] W. Balemans, N. Lounis, R. Gilissen, J. Guillemont, K. Simmen, K. Andries, A. Koul, *Nature* **2010**, *463*, E3–E5.

[13] M. Salmain, N. Metzler-Nolte, in: *Ferrocenes* (Ed.: P. Stepnicka), John Wiley and Sons, Chichester, **2008**, p. 499.

[14] a) C. G. Hartinger, P. J. Dyson, *Chem. Soc. Rev.* **2009**, *38*, 391–401; b) P. James, J. Neudörfl, M. Eissmann, P. Jesse, A. Prokop, H.-G. Schmalz, *Org. Lett.* **2006**, *8*, 2763–2766; c) N. I. Wenzel, N. Chavain, Y. Wang, W. Friebolin, L. Maes, B. Pradines, M. Lanzer, V. Yardley, R. Brun, C. Herold-Mende, C. Biot, K. Toth, E. Davioud-Charvet, *J. Med. Chem.* **2010**, *53*, 3214–3226; d) D. R. van Staveren, N. Metzler-Nolte, *Chem. Rev.* **2004**, *104*, 5931–5985; e) G. Jaouen (Ed.), *Bioorganometallics: Biomolecules, Labeling, Medicine*, Wiley-VCH, Weinheim, Germany, **2006**; f) G. Gasser, I. Ott, N. Metzler-Nolte, *J. Med. Chem.* **2011**, *54*, 3–25; g) E. A. Hillard, G. Jaouen, *Organometallics* **2011**, *30*, 20–27.

[15] a) L. Delhaes, C. Biot, L. Berry, P. Delcourt, L. A. Maciejewski, D. Camus, J. S. Brocard, D. Dive, *ChemBioChem* **2002**, *3*, 418–423; b) C. Biot, G. Glorian, L. A. Maciejewski, J. S. Brocard, O. Domarle, G. Blampain, P. Millet, A. J. Georges, H. Abessolo, D. Dive, J. Lebibi, *J. Med. Chem.* **1997**, *40*, 3715–3718.

[16] M. Patra, G. Gasser, M. Wenzel, K. Merz, J. E. Bandow, N. Metzler-Nolte, *Organometallics* **2010**, *29*, 4312–4319.

[17] J. B. Thomson, *Tetrahedron Lett.* **1959**, 26–27.

[18] K. P. Jang, C. H. Kim, S. W. Na, D. S. Jang, H. Kim, H. Kang, E. Lee, *Bioorg. Med. Chem. Lett.* **2010**, *20*, 2156–2158.

[19] a) K. Schlögl, H. Falk, *Angew. Chem.* **1964**, *76*, 570; b) K. Schlögl, H. Falk, *Monatsh. Chem.* **1965**, *96*, 266–275.

[20] O. Delacroix, B. Andriamihaja, S. Picart-Goetghelucka, J. Brocard, *Tetrahedron* **2004**, *60*, 1549–1556.

[21] H. Des Abbayes, R. Dabard, *Tetrahedron* **1975**, *31*, 2111–2116.

[22] M. E. Kuehne, W. Dai, Y.-L. Li, *J. Org. Chem.* **2001**, *66*, 1560–1566.

[23] J. McNulty, J. J. Nair, A. Capretta, *Tetrahedron Lett.* **2009**, *50*, 4087–4091.

[24] D. Apreutesei, G. Lisa, H. Akutsu, N. Hurduc, S. Nakatsuji, D. Scutaru, *Appl. Organomet. Chem.* **2005**, *19*, 1022–1037.

[25] U. T. Mueller-Westerhoff, R. W. Sanders, *Organometallics* **2003**, *22*, 4778–4782.

[26] C. S. Shiner, A. H. Berks, *J. Org. Chem.* **1988**, *53*, 5542–5545.

[27] P. Heretsch, A. Giannis, *Synthesis* **2007**, 2614–2616.

[28] G. M. Sheldrick, University of Göttingen, Germany, **1997**.

[29] A. L. Spek, *Acta Crystallogr., Sect. A: Found. Crystallogr.* **1990**, *46*, C34.

[30] B. Gautheron, R. Broussier, *Tetrahedron Lett.* **1971**, *12*, 513–516.

Received: May 15, 2011
Published Online: June 22, 2011

  